

A Second Species of the Rogadine Genus, *Batothecoides* Watanabe, 1958 (Hymenoptera: Braconidae) from Thailand

AVINJIKKATTU PARAMBIL RANJITH^{1,2}, DONALD L. J. QUICKE¹ AND BUNTIKA A. BUTCHER^{1*}

¹Integrative Insect Ecology Research Unit, Department of Biology, Faculty of Science, Chulalongkorn University, Phayathai Road, Pathumwan, Bangkok 10330, THAILAND

²Kālinga Foundation, Agumbe, Karnataka, INDIA

*Corresponding author. Buntika A. Butcher (buntika.a@chula.ac.th)

Received: 20 March 2025; Accepted: 13 June 2025; Date of publication: 14 October 2025
https://zoobank.org/urn:lsid:zoobank.org:pub: 394B5675-7419-498D-A21D-7383021D33A7

ABSTRACT.— A second species of the rogadine braconid wasp genus, *Batothecoides* Watanabe, 1958 is described from Thailand, the genus having been known only from the type species for the past 66 years. The new species, *Batothecoides sirindhornae* Ranjith, Butcher & Quicke, sp. nov., is distinguished from the type species of the genus, *B. yakushimensis* (Watanabe, 1938), by morphology, color and DNA sequence data. The type species is redescribed based on images of the holotype. A molecular phylogeny of all members of the subtribe Spinariina for which barcode data are available is presented.

KEYWORDS: *Spinaria*, Oriental region, molecular data, redescription

INTRODUCTION

The rogadine subtribe Spinariina comprises six genera distributed across the Oriental, East Palaearctic and Australasian regions (van Achterberg, 2007; Quicke et al., 2021; Gupta et al., 2024). Initially, this group was treated as a tribe (Spinariini van Achterberg, 1988), defined by the presence of spine-like projections from the metasomal carapace and tergites. This classification followed the inclusion of *Spinaria* Brullé 1846, *Batothecoides* Watanabe, 1958, and *Batotheca* Enderlein, 1905 (van Achterberg, 1988). Subsequently, molecular data and morphological evidence led to the inclusion of three additional genera—*Spinariella* Szépligeti, 1906, *Conspinaria* Schulz, 1906, and *Cornuto-rogas* Chen, Belokobylskij, van Achterberg & Whitfield, 2004—in this group, which van Achterberg (2007) treated as a subtribe. Several molecular studies have now confirmed the monophyly of this subtribe and/or placed it in the Rogadini, specifically as sister group to *Rogas* Nees, 1819 (Jasso-Martínez et al., 2020; Zaldivar-Riverón et al., 2004, 2006; Quicke et al., 2021; Shimbori et al., 2024). The group is further informally divided into the *Spinaria* subgroup, which have an elongate pronotum and mesoscutum, a normal mesosoma in lateral view, and the tarsal claws with a lobe or lamella, and the *Batotheca* subgroup, with a short pronotum and a robust mesoscutum, a dorso-ventrally enlarged mesosoma in lateral view, and the tarsal claws without a lobe or lamella (van Achterberg, 2007).

The genus *Batothecoides* can be distinguished by the following combination of characters: occipital carina present and complete; first metasomal tergite immovably fused with the second tergite; pronotum without a spine; and the metanotum without a medial

protuberance (van Achterberg, 2007). The genus was described by Watanabe (1958) for *Batotheca yakushimensis* Watanabe, 1938, which until now remained the only known species of *Batothecoides*, which has been reported from the Eastern Palaearctic and Oriental regions (Watanabe, 1938; Yu et al., 2016). In this study we describe and illustrate a second species from Thailand, 66 years after the description of the type species. We provide a COI DNA barcode and maximum likelihood tree for the species of Spinariina along with a redescription of the type species of *Batothecoides* based on images of the holotype.

MATERIALS AND METHODS

The single specimen of the new species was collected at the Sakaerat Environmental Research Station, Thailand. The holotype of the new species is deposited in the Insect Museum, Chulalongkorn University Museum of Natural History, Bangkok, Thailand (CUMZ). Morphological terminology follows van Achterberg (1993); for cuticular sculpture we follow Harris (1979). Images of the new species were taken using a Leica M205 C Stereozoom trinocular microscope and stacked using LAS X software.

A sequence for the barcoding region of cytochrome oxidase c subunit 1 (COI) was generated from a single leg by the Centre for Biodiversity Genomics, University of Guelph, based on standard protocols as described in Hebert et al. (2003), Park et al. (2010), and Quicke et al. (2021). Alignment was trivial as there were no indels. A molecular data matrix was created for all species of the subtribe Spinariina plus three species of its sister genus *Rogas*, for rooting. Provenances of sequenced specimens, DNA barcode index

TABLE 1. Specimens used for molecular analysis with their provenances and GenBank accession numbers.

Species	Provenance	Voucher code	Process id	BOLD:BIN	GenBank Accession no.
<i>Batotheca</i> sp.	Papua New Guinea	USNM:ENT:00680162a	ASQSP017-08	AAI4667	JF415904
<i>Batothecoides</i>	Thailand	CCDB-47581-A03	BBTH6555-24	AGN6535	PQ662811
<i>sirindhornae</i> sp. nov.					
<i>Batothecoides</i>	China	BCLDQR-00030	ASQSP118-08	AAP5878	JF962970
<i>yakushimensis</i>					
<i>Conspinaria</i> sp. 1	Taiwan	AZR-2008	-	-	EU480586
<i>Conspinaria</i> sp. 7	Taiwan	BF02599	ASQBR1003-20	-	MT806391
<i>Conspinaria</i> sp.	Thailand	BF-0000633	ASQAS227-11	AAS0085	EU979612
<i>Conspinaria</i> sp.	Thailand	BF002409	ASQAS228-11	AAU7351	JF963139
<i>Cornutorogas</i> sp.	Thailand	BCLDQ00164	ASQSP416-08	AAI5891	JF963141
<i>Cornutorogas</i> sp.	Thailand	BCLDQ00149	ASQSP401-08	AAG7577	MT639374
<i>Cornutorogas</i> sp.	Thailand	BCLDQ00157	ASQSP409-08	AAH8673	MT639384
<i>Cornutorogas</i> sp.	Thailand	BCLDQ0223	ASQSP193-08	AAG7568	MT639426
<i>Cornutorogas</i> sp.	Thailand	BCLDQ0763	ASQSQ044-09	AAI5892	MT639434
<i>Spinaria sundana</i>	Thailand	CCDB-47579-E09	BBTH6419-23	AAG2674	-
<i>Spinaria</i> sp.	Papua New Guinea	USNM:ENT:00680079	ASQSP030-08	AAG2673	JF271524
<i>Spinaria</i> sp.	Thailand	BCLDQ01653	ASQSR217-11	AAV3411	JN278378
<i>Spinaria</i> sp. nr <i>sundana</i>	Thailand	BCLDQ01657	ASQSR221-11	AAG2674	JN278382
<i>Spinaria flavipennis</i>	Thailand	CCDB-32186-H11	BBTH3227-22	AAV3411	-
<i>Spinaria vietnamica</i>	Thailand	BCLDQ01655	ASQSR219-11	AAJ3616	JN278380
<i>Rogas luteus</i>	France	CNIN200	GBAHB1289-15	ACS4625	KM067264
<i>Rogas nigrovenosus</i>	Russia	CNIN3895	ASQBR1007-23	AEK0049	ON101910
<i>Rogas roxana</i>	Russia	CNIN5100	-	-	PP719462

numbers (BINs), and GenBank accession numbers are given in Table 1.

We conducted Maximum Likelihood analysis for the gene fragment COI using IQTREE v2.1.3 (Minh et al., 2020). The best-fit model, determined by Model Finder (Kalyaanamoorthy et al., 2017) based on the corrected Akaike Information Criterion (AICc), was GTR+F+I+R2. Branch support was estimated with 1,000 ultrafast bootstraps (Hoang et al., 2018). The tree was visualised using FigTree v. 1.4.4. (Rambaut, 2018).

RESULTS

Systematics

Batothecoides Watanabe, 1958

Batothecoides Watanabe, 1958: 53; Shenefelt, 1975: 1186. Type species: *Batotheca yakushimensis* Watanabe, 1938.

Diagnosis.— Occipital carina present, complete. Head directly narrowed behind eyes and comparatively small, much narrower than mesoscutum. Eyes distinctly emarginate near level of antennal sockets. Notauli complete and including medio-posterior depression. Metanotum not protruding dorsally, but propodeum protruding anteriorly. Vein r of fore wing emitted in front of middle of pterostigma. Vein $m-cu$ of

hind wing absent. vein $cu-a$ of hind wing long and moderately reclivous. Tarsal claws simple. First metasomal tergite immovably joined to second tergite and with large dorsope, its dorsal carinae far separated from each other throughout, without a median carina. Second tergite without a semi-circular area medio-basally. First-fifth tergites with acute lateral margin; third-fifth tergites with obtuse teeth. Fifth tergite strongly convex subbasally and with a pair of medio-posterior teeth. Ovipositor sheath medium-sized, narrow, not widened subapically.

Notes.— No significant sexual dimorphism is observed between male and female specimens of the type species, *B. yakushimensis*, as van Achterberg (2007) only noted a color difference in the anterior part of the propodeum.

Distribution.— East Palaearctic and Oriental regions.

Biology.— Unknown.

Batothecoides sirindhornae Ranjith, Butcher & Quicke sp. nov.

(Figs 1–3)

<https://zoobank.org/urn:lsid:zoobank.org:act:60335FD1-9B4B-4AD0-A802-D2DEB82BF3C8>

Etymology.— The new species is named in honour of H.R.H. Princess Maha Chakri Sirindhorn of Thailand in celebration of the year of her seventieth birthday.



FIGURE 1. *Batothecoides sirindhornae* sp. nov. holotype, male **A.** habitus, lateral view; **B.** head, anterior view; **C.** head, dorsal view; **D.** head, lateral view; **E.** head, dorso-ventral view.



FIGURE 2. *Batothecoides sirindhornae* sp. nov. holotype, male **A**. head, oblique view; **B**. mesosoma, lateral view; **C**. mesosoma, dorsal view; **D**. propodeum, dorsal view; **E**. metasoma, lateral view; **F**. metasomal tergite 1, dorsal view.

Material examined.— Holotype, male, THAILAND: Nakhon Ratchasima, Wang Nam Khiao, Udom Sap, Sakaerat Environmental Research Station (SERs), 14°49.672'N, 101°91.615'E, 496 masl, 3.x.2023, coll.

S. Boonyong & K. Chansri (CUMZ) (with following DNA data: sample ID CCDB-47581-A03, BOLD Process ID BBTH6555-24, BIN ID: BOLD:AGN6535; Genbank accession: COI PQ662811).



FIGURE 3. *Batothecoides sirindhorna* sp. nov. holotype, male **A.** metasoma, dorsal view; **B.** metasomal tergites 3–5, dorsal view; **C.** metasomal tergites 4–5, oblique view; **D.** hind tarsal claw, lateral view; **E.** wings.

Diagnosis.— The new species differs from the only other described other known species of *Batothecoides*, *B. yakushimensis*, by the following characters: metasomal tergites 4–5 blackish brown (ivory in *B. yakushimensis*); hind tarsomeres 1–4 yellow (black in *B.*

yakushimensis); hind femur 3.7 × as long as wide (4.3 × in *B. yakushimensis*); lateral protuberances of metasomal tergite 3 prominent (not prominent in *B. yakushimensis*); submedial longitudinal carinae on dorsal pronotum anteriorly diverging (parallel in *B. yakushimensis*).

sis); and hind basitarsus $4.1 \times$ as long as wide ($6.2 \times$ in *B. yakushimensis*).

Description.— Holotype, male, length of body 11.2 mm, of fore wing 9.2 mm.

Head. Antenna with 44 segments and $1.1 \times$ as long as fore wing, length of third segment $1.1 \times$ as long as fourth segment, third, fourth and penultimate segments 1.1, 1.1 and $2.2 \times$ as long as wide respectively; head $1.3 \times$ as wide as high anterior view, $1.6 \times$ as wide as long in dorsal view; face smooth with long setae, $1.4 \times$ as wide as high (Fig. 1B); maxillary palp with five segments, second and third segments bulging (Fig. 1D); labial palp with four segments (Fig. 1D); length of maxillary palp $0.8 \times$ height of head, frons slightly depressed medially and smooth (Fig. 1C); OOL: diameter of posterior ocellus: POL = 1.0:1.2:1.0; vertex narrow dorsally, strongly declivous, smooth and shiny (Figs 1C–E, 2A); occipital carina complete, strong (Figs 1C–E, 2A); length of eye $1.5 \times$ temple in dorsal view; temple and back of head with comparatively long setae (Figs 1C–E, 2A); clypeus smooth, medio-ventral rim of clypeus slightly above lower level of eyes (Fig. 1B); length of malar space $0.8 \times$ basal width of mandible and $0.3 \times$ height of eye in lateral view; width of face $2.0 \times$ width of hypoclypeal depression, $0.8 \times$ height of eye and equal to height of face and clypeus combined.

Mesosoma. Length of mesosoma $1.2 \times$ longer than its height; pronotum dorsally distinctly convex, antero-medially concave with a pair of raised carina sub-medially, and antero-laterally with shallow depression (Fig. 2C); mesoscutal lobes smooth and setose except middle lobe of mesoscutum irregularly sculptured anteriorly (Fig. 2C); notauli complete and crenulate, meeting posteriorly, medio-posterior depression deep, bordered with longitudinal carinae (Fig. 2C); scutellar sulcus with three coarse carinae and about $0.7 \times$ as long as scutellum (Fig. 2C); scutellum nearly flat and smooth, setose, except for a few punctures (Fig. 2C); prepectal carina with wide crenulations medially (Figs 1A, 2B); mesopleuron punctate anteriorly, smooth and glabrous medially, coarsely rugose posteriorly with a protuberance posteriorly (Figs 1A, 2B); precoxal sulcus crenulate (Figs 1A, 2B); mesosternal sulcus distinctly crenulate and rather deep; metapleuron coarsely rugose, setose (Figs 1A, 2B); metanotum crenulate (Fig. 2D); propodeum coarsely reticulate-rugose with antero-medial acute protuberance, no distinct median carina and laterally with a pair of small smooth convexities, posteriorly with a pair of short midlongitudinal carinae (Fig. 2D).

Wings. Fore wing (Fig. 3E): r thicker than 3-SR and

straight; r:3-SR:SR1 = 1.0: 2.2: 4.7; 1-CU1:2-CU1 = 1.0: 4.2; 2-SR:3-SR:r-m = 1.0: 1.5: 1.1; cu-a postfurcal, subvertical; m-cu antefurcal. Hind wing (Fig. 3E): marginal cell subparallel-sided apically, 1r-m straight; M+CU:1-M:1r-m = 2.0: 1.6: 1.0; 2-SC+R subquadrate; cu-a long and sinuate.

Legs. Hind coxa rather densely setose and moderately punctate, postero-dorsally flattened and with short oblique crenulae (Fig. 1A); tarsal claws simple (Fig. 3D); length of femur, tibia and basitarsus of hind leg 3.7, 7.0 and $4.1 \times$ their width, respectively; hind tarsus long bristly setose; length of hind tibial spurs 0.3 and $0.4 \times$ hind basitarsus; hind tarsus $0.8 \times$ as long as hind tibia.

Metasoma. Metasomal tergite 1 coarsely reticulate-rugose with a pair of posteriorly converging medial longitudinal carinae, longitudinally striate-rugose medio-posteriorly, length of metasomal tergite 1 $0.7 \times$ as long as its apical width (Fig. 2E, F); metasomal tergite 2 longitudinally striate-rugose medially, rest reticulate-rugose, $2.1 \times$ as wide as long (Fig. 3A); metasomal tergite 3 longitudinally striate-rugose, $2.8 \times$ as wide as long (Fig. 3A); metasomal tergites 3–5 with lateral acute, rounded lobes (Fig. 3A–C); metasomal tergites 4–5 coarsely reticulate-rugose associated with irregular longitudinal carinae (Fig. 3A–C); metasomal tergite 5 strongly convex anteriorly, with a pair of apically rounded medio-posterior teeth (Fig. 3A–C).

Color. Body yellow except antenna, apex of mandible, eye, ocellar triangle, lateral lobes of mesoscutum, propodeum, fore wing veins and pterostigma, hind leg except tarsomeres 1–4, metasomal tergite 1 medio-posteriorly, tergite 2 except laterally, tergites 3–5 blackish brown; medial lobe of mesoscutum, mesopleuron ventrally, posterior band of scutellum, propodeum antero-medially reddish brown; tergite 1 except medio-posteriorly, tergite 2 laterally, tergite 3 antero-laterally ivory.

Distribution.— Thailand

Biology.— Unknown

***Batothecoides yakushimensis* (Watanabe, 1938)**
(Figs 4–6)

Batotheca yakushimensis Watanabe, 1938: 173.

Batothecoides yakushimensis; Watanabe, 1958: 53;

Shenefelt, 1975: 1186; van Achterberg, 2007: 66.

Material examined (holotype images).— Holotype, ♀, “[Japan, Kyushu, Yakushima], Onoaida, 2.viii.1929, Hiroshi Hori” (Kyushu University, Fukuoka).

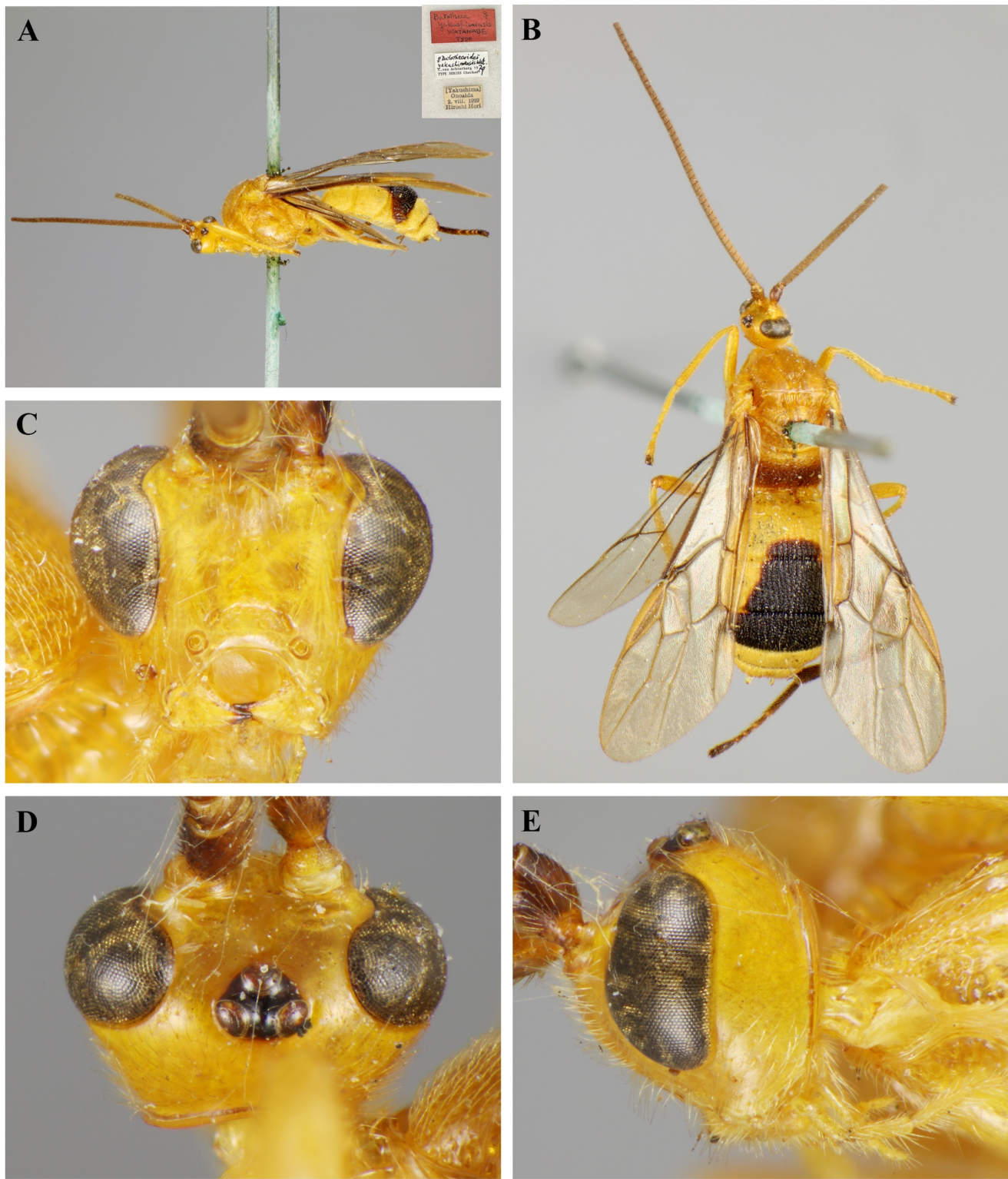


FIGURE 4. *Batothecoides yakushimensis* (Watanabe, 1938), holotype, female **A.** habitus, lateral view; **B.** habitus, dorsal view; **C.** head, anterior view; **D.** head, dorsal view; **E.** head, lateral view.

Redescription.—Holotype, length of body 9.1 mm of fore wing 8.4 mm.

Head. Antenna incomplete with 46 segments, length of third segment 1.3 \times as long as fourth segment, third, fourth segments 1.1 and 0.9 \times as long

as wide respectively; head 1.3 \times as wide as high anterior view, 1.4 \times as wide as long in dorsal view; face smooth with long setae, 1.5 \times as wide as long (Fig. 4C); maxillary palp with five segments (Fig. 4E); labial palp with four segments (Fig. 4E); length of maxillary

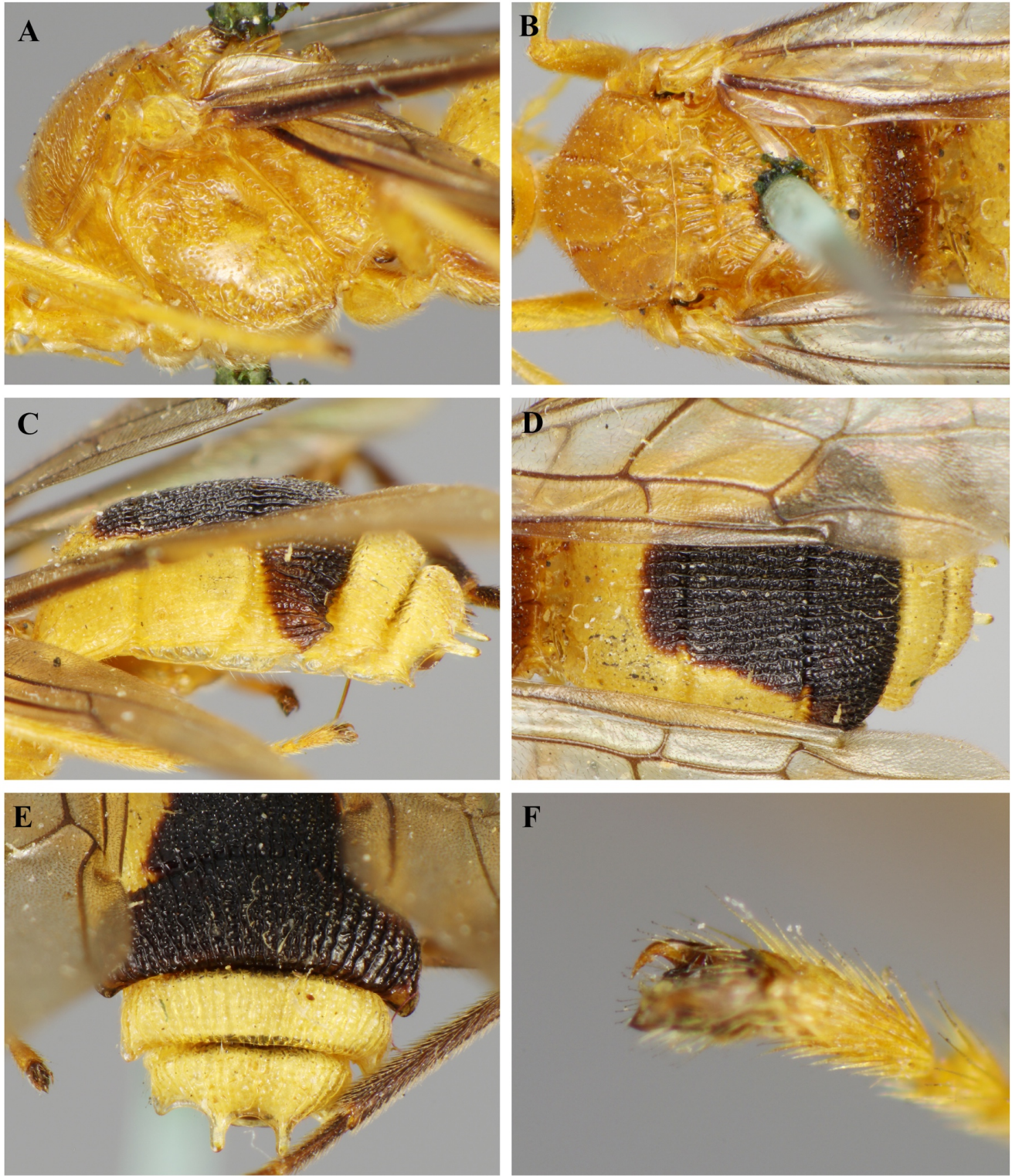


FIGURE 5. *Batothecoides yakushimensis* (Watanabe, 1938), holotype, female. **A.** mesosoma, lateral view; **B.** mesosoma, dorsal view; **C.** metasoma, lateral view; **D.** metasoma, dorsal view; **E.** metasomal tergite 3–5, dorsal view; **F.** hind tarsal claw, lateral view.

palp $0.9 \times$ height of head; frons slightly depressed medially and smooth (Fig. 4D); OOL: diameter of posterior ocellus: POL = 1.9: 1.7: 1.0; vertex narrow dorsally, strongly declivous, smooth and shiny (Fig. 5D); occipital carina complete, strong (Fig. 4D, E);

length of eye $0.8 \times$ temple in dorsal view; temple and back of head comparatively long setose (Fig. 4D); clypeus smooth, medio-ventral rim of clypeus slightly above lower level of eyes (Fig. 4C); length of malar space $1.2 \times$ basal width of mandible and $0.3 \times$ height of

eye in lateral view; width of face $1.9 \times$ width of hypoclypeal depression, $0.9 \times$ height of eye and $1.1 \times$ height of face and clypeus combined.

Mesosoma. Length of mesosoma $1.3 \times$ longer than its height; pronotum dorsally distinctly convex, antero-medially concave with a pair of raised carinae submedially and antero-laterally with shallow depression; mesoscutal lobes smooth and setose except middle lobe of mesoscutum irregularly sculptured anteriorly (Fig. 5B); notaui complete and crenulate, meeting posteriorly, medio-posterior depression deep, bordered with longitudinal carinae (Fig. 5B); scutellar sulcus with five coarse carinae and about $0.5 \times$ as long as scutellum (Fig. 5B); scutellum nearly flat and smooth, setose, except for a few punctures (Fig. 5B); prepectal carina with wide crenulations medially (Figs 4A, 5A); mesopleuron punctate anteriorly, with small smooth glabrous area medially, coarsely rugose posteriorly with a protuberance posteriorly (Figs 4A, 5A); precoxal sulcus crenulate (Figs 4A, 5A); mesosternal sulcus distinctly crenulate and rather deep; metapleuron coarsely rugose, setose (Figs 4A, 5A); metanotum crenulate; propodeum coarsely reticulate-rugose with antero-medial acute protuberance (Fig. 5B).

Wings. Fore wing (Fig. 4B): r moderately thicker than 3-SR and straight; r:3-SR:SR1 = 1.0: 2.6: 4.6; 1-CU1:2-CU1 = 1.0: 5.0; 2-SR:3-SR:r-m = 1.2: 2.4: 1.0; cu-a postfurcal, subvertical; m-cu antefurcal. Hind wing (Fig. 4B): marginal cell subparallel-sided apically, 1r-m straight; M+CU:1-M:1r-m = 2.8: 1.8: 1.0; 2-SC+R subquadrate; cu-a long and sinuate.

Legs. Hind coxa rather densely setose and moderately punctate, postero-dorsally flattened and with short oblique crenulae (Fig. 1A); tarsal claws simple (Fig. 5F); length of femur, tibia and basitarsus of hind leg 4.3, 7.4 and $6.2 \times$ their width, respectively; hind tarsus long bristly setose; length of hind tibial spurs $0.3 \times$ as long as hind basitarsus; hind tarsus $0.8 \times$ as long as hind tibia.

Metasoma. Metasomal tergite 1 coarsely reticulate-rugose with a pair of posteriorly converging medial longitudinal carinae, longitudinally striate-rugose medio-posteriorly, length of metasomal tergite 1 $0.6 \times$ as long as its apical width (Fig. 5C, D); tergite 2 longitudinally striate-rugose medially, rest reticulate-rugose, $2.6 \times$ as wide as long (Fig. 5D); tergite 3 longitudinally striate-rugose, $2.7 \times$ as wide as long (Fig. 3A); tergites 3–5 with lateral acute, short, rounded lobes (Fig. 5D, E); tergites 4–5 coarsely reticulate-rugose associated with irregular longitudinal carinae (Fig. 5C–E); tergite 5 strongly convex anteriorly, with a pair of apically rounded medio-posterior teeth (Fig. 5E).

Color. Body mostly yellow except antenna, apex of mandible, eye, ocellar triangle, propodeum except anterior 1/3, fore wing veins and pterostigma; hind leg, metasomal tergite 1 medio-posteriorly, tergite 2 except laterally blackish brown, mesoscutum, mesopleuron ventrally, posterior band of scutellum, metasomal tergite 1 except medio-posteriorly, tergite 2 laterally, tergite 3 antero-laterally ivory.

Male.— Similar as female except anterior half of propodeum yellowish brown (van Achterberg, 2007).

Distribution.— China and Japan.

Biology.— Unknown.

Molecular results

The four included Spinariina genera represented by more than one species were recovered as monophyletic with $>90\%$ ultrarapid bootstrap support. The genus level topology places *Batothecoides* as sister group to all other Spinariina. However, none of the intergeneric relationships were robustly supported.

DISCUSSION

Apart from the distinct morphological differences, our molecular data confirmed the distinctiveness of *B. sirindhornae* sp. nov. from *B. yakushimensis*, their 658 base pair DNA barcodes differing at 45 base positions (i.e. 6.84%), whereas most workers consider a 2% difference to indicate that specimens probably belong to different species (Hebert et al., 2003; Meyer and Paulay, 2005; Hubert et al., 2008; Rivera and Currie, 2009; Stoeckle and Thaler, 2014; Hubert and Hanner, 2015). A DNA barcode gap of 6% in insects suggests an approximate divergence time of approximately 10–20 million years, although this is a rough estimate and a more accurate assessment would require many more sequences and fossil calibration which is currently not possible because there are no known fossils of any Spinariina or other Rogadinae.

Morphologically the subtribe Spinariina divides into two groups: the *Spinaria* subgroup ((*Spinaria*, *Spinariella*, *Conspinaria*, *Cornutorogas*) and *Batotheca* subgroup (*Batotheca*, *Batothecoides*) (van Achterberg, 2007). The former possesses an elongate pronotum and mesoscutum, a normal mesosoma in lateral view, and tarsal claws usually with a well-developed basal lobe whereas members of the latter have an unmodified short pronotum and a robust mesoscutum and their claws lack a pointed or angular basal lobe. However, a molecular phylogenetic study of the Rogadinae based

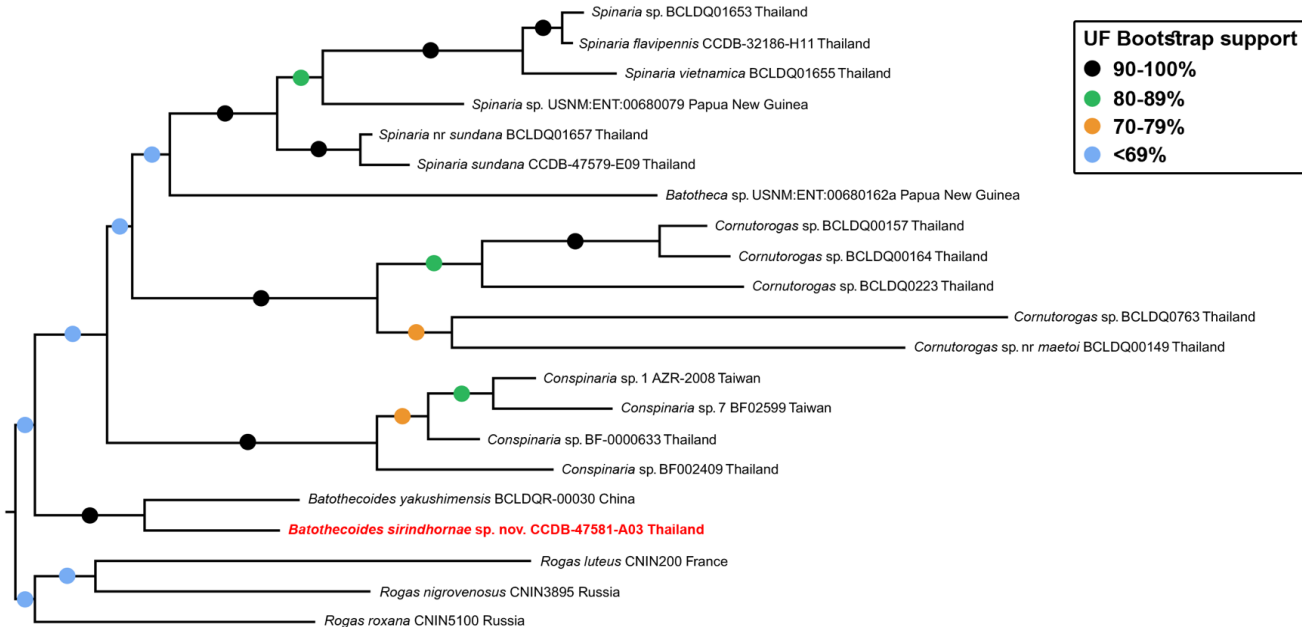


FIGURE 6. Maximum Likelihood tree of the subtribe Spinariina based on COI gene fragment. Support values at nodes are rapid bootstrap and indicated by colored dots.

on four gene fragments (including COI) instead recovered a quite different set of relationships, i.e., ((*Batothecoides*+*Conspinaria*), (*Cornutorogas*+(*Batotheca*+*Spinaria*))) (Quicke et al., 2021).

Our present single gene study differed from both of the above hypotheses but it should be noted that none of the inter-generic relationships here were supported by (>70%) although all genera were supported as monophyletic with 90–100% support.

Sexual dimorphism in the superfamily Ichneumonoidea is mostly associated with body size and coloration, and female and male specimens are generally quite similar (Quicke, 2015). Sexual dimorphism in *Batothecoides* is negligible and, for the type species, van Achterberg (2007) noted only a slight difference in coloration of the anterior part of the propodeum, which is yellowish brown in males compared to yellow in females. This is quite different from the situation in the rogadine genus *Troporogas* Cameron, 1905 in which there is very marked sexual colour dimorphism (Quicke et al., 2024).

ACKNOWLEDGEMENTS

We thank Mr Kittipum Chansri for the donation of the specimen. APR and DLJQ were supported by a postdoctoral fellowship from the Rachadaphisek-somphot Fund, Graduate School, Chulalongkorn University. We thank Dr Toshiharu Mita (Kyushu University, Japan) for sending the holotype images of *B.*

yakushimensis. We are grateful to Prof. Paul D.N. Hebert and the CCDB for sequencing support. This research is financially supported by Thailand Science Research and Innovation Fund Chulalongkorn University and Chulalongkorn University, Rachadaphisek-somphot Fund (RU66_008_2300_002) and RSPG Chula to BAB.

LITERATURE CITED

Areekul, B., Mori, M., Zaldivar-Riverón, A. and Quicke, D.L.J. 2005. Molecular and morphological phylogeny of the parasitic wasp genus *Yelicones* (Hymenoptera: Braconidae: Rogadinae). European Journal of Entomology, 102: 617–624. <https://doi.org/10.14411/eje.2005.087>

Gupta, A., van Achterberg, C., Reddy, P.M. and Sushil, S.N. 2024. Review of the subtribe Spinariina van Achterberg (Hymenoptera: Braconidae: Rogadinae) from India with description of one new species. Zootaxa, 5399: 347–364. <https://doi.org/10.11646/zootaxa.5399.4.3>

Harris, R.A. 1979. A glossary of surface sculpturing. Occasional Papers in Entomology of the California Department of Food and Agriculture, 28: 1–31.

Hebert, P.D.N., Cywinski, A., Ball, S.L. and deWaard, J.R. 2003. Biological identifications through DNA barcodes. Proceedings of the Royal Society of London Series B: Biological Sciences, 270: 313–321. <https://doi.org/10.1098/rspb.2002.2218>

Hoang, D.T., Chernomor, O., Von Haeseler, A., Minh, B.Q. and Vinh, L.S. 2018. UFBoot2: improving the ultrafast bootstrap approximation. Molecular Biology and Evolution, 35(2): 518–522. <https://doi.org/10.1093/molbev/msx281>

Hubert, N. and Hanner, R. 2015. DNA Barcoding, species delineation and taxonomy: a historical perspective. DNA Barcodes, 3(1): 44–58. <https://doi.org/10.1515/dna-2015-0006>

Hubert, N., Hanner, R., Holm, E., Mandrak, N. E., Taylor, E., Burridge, M., Watkinson, D., Dumont, P., Curry, A., Bentzen, P., Zhang, J., April, J. and Bernatchez L. 2008. Identifying Canadian freshwater fishes through DNA barcodes. *PLoS ONE*, 3: e2490. <https://doi.org/10.1371/journal.pone.0002490>

Jasso-Martínez, J.M., Quicke, D.L.J., Belokobylskij, S.A., Meza-Lázaro, R.M. and Zaldívar-Riverón, A. 2020. Phylogenomics of the lepidopteran endoparasitoid wasp subfamily Rogadinae (Hymenoptera: Braconidae) and related subfamilies. *Systematic Entomology*, 46: 83–95. <https://doi.org/10.1111/syen.12449>

Kalyaanamoorthy, S., Minh, B.Q., Wong, T.K.F., von Haeseler, A. and Jermiin. L.S. 2017. ModelFinder: fast model selection for accurate phylogenetic estimates. *Nature Methods*, 14: 587–589. <https://doi.org/10.1038/nmeth.4285>

Meyer, C.P. and Paulay, G. 2005. DNA barcoding: error rates based on comprehensive sampling. *PLoS Biology*, 3: e422. <https://doi.org/10.1371/journal.pbio.0030422>

Minh, B.Q., Schmidt, H.A., Chernomor, O., Schrempf, D., Woodhams, M.D., von Haeseler, A. and Lanfear, R. 2020. IQ-TREE 2: new models and efficient methods for phylogenetic inference in the genomic era. *Molecular Biology and Evolution*, 37: 1530–1534. <https://doi.org/10.1093/molbev/msaa015>

Park, D.S., Suh, S.J., Oh, H.W. and Hebert, P.D.N. 2010. Recovery of the mitochondrial COI barcode region in diverse Hexapoda through tRNA-based primers. *BMC Genomics*, 11: 1–7. <https://doi.org/10.1186/1471-2164-11-423>

Quicke, D.L.J. 2015. Biology, systematics, evolution and ecology of braconid and ichneumonid parasitoid wasps. Chichester: Wiley Blackwell, p. 688.

Quicke, D.L.J., Fagan-Jeffries, E.P., Jasso-Martínez, J.M., Zaldívar-Riverón, A., Shaw, M.R., Janzen, D.H., Hallwachs, W., Smith, M.A., Hebert, P.D.N., Hrcek, J., Miller, S., Sharkey, M.J., Shaw, S.R. and Butcher, B.A. 2021. A molecular phylogeny of the parasitoid wasp subfamily Rogadinae (Ichneumonoidea: Braconidae) with descriptions of three new genera. *Systematic Entomology*, 46: 1019–1044. <https://doi.org/10.1111/syen.12507>

Quicke, D.L.J., Ranjith, A.P., Loncle, M.K., van Achterberg, C., Long, K.D. and Butcher, B.A. 2024. Revision of *Troporhogas* Cameron (Hymenoptera, Braconidae, Rogadinae) with six new species from India and Thailand. *ZooKeys*, 1206: 99–136. <https://doi.org/10.3897/zookeys.1206.120824>

Rambaut, A. 2016. FigTree v1.4.3. <http://tree.bio.ed.ac.uk/software/figtree/>

Rivera, J. and Currie, D.C. 2009. Identification of Nearctic black flies using DNA barcodes (Diptera: Simuliidae). *Molecular Ecology Resources*, 9: 224–236. <https://doi.org/10.1111/j.1755-0998.2009.02648.x>

Shimbori, E.M., Castañeda-Osorio, R., Jasso-Martínez, J.M., Penteado-Dias, A.M., Gadelha, S.S., Brady, S.G., Quicke, D.L.J., Kula, R. and Zaldívar-Riverón, A. 2024. UCE-based phylogenomics of the lepidopteran endoparasitoid wasp subfamily Rogadinae (Hymenoptera: Braconidae) unveils a new Neotropical tribe. *Invertebrate Systematics*, 38(8): IS24040. <https://doi.org/10.1071/IS24040>

Stoeckle, M.Y. and Thaler, D.S. 2014. DNA barcoding works in practice but not in (neutral) theory. *PLoS ONE*, 9: e100755. <https://doi.org/10.1371/journal.pone.0100755>

van Achterberg, C. 1988. Parallelisms in the Braconidae (Hymenoptera) with special reference to the biology, 85–115, In: Gupta, V.K. (ed.) *Advances in Parasitic Hymenoptera Research*, E. J. Brill Publishers, Inc., Kinderhook, N.Y. USA. 546 pp.

van Achterberg, C. 1993. Illustrated key to the subfamilies of the Braconidae (hymenoptera: Ichneumonoidea). *Zoologische Verhandelingen*, Leiden, 283: 1–189.

van Achterberg, C. 2007. Revision of the genus *Spinaria* Brullé (Hymenoptera: Braconidae: Rogadinae), with keys to genera and species of the subtribe Spinariina van Achterberg. *Zoologische Mededelingen*, Leiden, 81: 11–83.

Watanabe, C. 1938. A revision of the genus *Batotheca* Enderlein, with description of a new species (Hym., Braconidae). *Mushi*, 11: 170–175.

Watanabe, C. 1958. Further revisions of *Spinaria* Brullé and *Batotheca* Enderlein, with description of a new genus (Hymenoptera, Braconidae). *Acta Hymenopterologica*, 1: 51–53.

Yu, D.S.K., van Achterberg, C. and Horstmann, K. 2016. Taxapad 2016. Ichneumonoidea 2015. Taxapad, Nepean, Ontario. [database on flash-drive]

Zaldívar-Riverón, A., Areekul, B., Shaw, M.R. and Quicke, D.L.J. 2004. Comparative morphology of the venom apparatus in the braconid wasp subfamily Rogadinae (Insecta, Hymenoptera, Braconidae) and related taxa. *Zoologica Scripta*, 33: 223–238. <https://doi.org/10.1111/j.0300-3256.2004.00144.x>

Zaldívar-Riverón, A., Mori, M. and Quicke, D.L.J. 2006. Systematics of the cyclostome subfamilies of braconid parasitic wasps (Hymenoptera: Ichneumonoidea): a simultaneous molecular and morphological Bayesian approach. *Molecular Phylogenetics & Evolution*, 38: 130–145. <https://doi.org/10.1016/j.ympev.2005.08.006>